An Agent-Based Hierarchical Bargaining Framework for Power Management of Multiple Cooperative Microgrids

Authors: Kaveh Dehghanpour & Hashem Nehrir

Dehghanpour, Kaveh, and Hashem Nehrir. “An Agent-Based Hierarchical Bargaining Framework for Power Management of Multiple Cooperative Microgrids.” IEEE Transactions on Smart Grid 10, no. 1 (January 2019): 514–522. doi:10.1109/tsg.2017.2746014.

An Agent-Based Hierarchical Bargaining Framework for Power Management of Multiple Cooperative Microgrids

Kaveh Dehghanpour, *Student Member, IEEE,* Hashem Nehrir, *Life Fellow, IEEE,*

***Abstract*—In this paper, we propose an agent-based hierarchical power management model in a power distribution system composed of several MicroGrids (MGs). At the lower level of the model, multiple MGs bargain with each other to cooperatively obtain a fair, and Pareto-optimal solution to their power management problem, employing the concept of Nash Bargaining Solution (NBS) and using a distributed optimization framework. At the highest level of the model, a distribution system power supplier, e.g. a utility company, interacts with both the cluster of the MGs and the wholesale market. The goal of the utility company is to facilitate power exchange between the regional distribution network consisting of multiple MGs and the wholesale market to achieve its own private goals. The power exchange is controlled through dynamic energy pricing at the distribution level, at the day-ahead and real-time stages. To implement energy pricing at the utility company level, an iterative machine learning mechanism is employed, where the utility company develops a price-sensitivity model of the aggregate response of the MGs to the retail price signal through a learning process. This learned model is then used to perform optimal energy pricing. To verify its applicability, the proposed decision model is tested on a system with multiple MGs, with each MG having different load/generation data.**

***Index Terms*—Microgrids, bargaining games, distributed optimization, agent-based modeling, power management.**

I. Introduction

MicroGrids (MGs), as small-scale self-sustainable energy units, represent an attractive opportunity for large-scale integration of renewable and non-renewable micro-sources into power distribution systems. However, as the number of MGs in Regional Energy Networks (RENs) grows, developing control and power management logics to coordinate the operation of MGs and facilitate their constructive interaction becomes crucial. Also, it is critical to design retail market mechanisms considering the autonomy of MGs in the regional distribution networks. Noting that MGs introduce higher levels of controllability and price-aware functionalities into the system, the effect of their increasing penetration on retail market operation will no longer be negligible.

Several papers have addressed different aspects of the problem of controlling and energy management of power systems with multiple MGs. In [1], a frequency reserve provision procedure is proposed using a market mechanism including several MGs. Different control strategies are examined in order to enable the participation of renewable resources in frequency control. In [2] and [3], using auction theory a two-level market framework is developed to facilitate power trading among multiple MGs. The proposed auctions are based on control agents that participate in local and global markets through bidding. In [4], another bi-level decision hierarchy is proposed. At the local level total cost minimization for each MG is addressed, while at the upper level a central control unit is in charge of coordinating multiple MGs to balance power and prevent excess/shortage of power at the global level. In [5], charging management of electric vehicles in a multi-MG environment is studied using a decentralized price-based strategy. In [6], the problem of cooperation among several MGs using a hierarchical scheduling approach, exploiting MG diversity gain to optimize performance and user satisfaction is addressed. In [7], using Stackelberg game model, a distributed framework is proposed to design trading processes among several MGs. In [8], a distributed-optimization-based model is proposed with the objective of minimizing the total operational cost of multiple MGs.

This paper is the extension of our earlier work, [9], where we extend the agent-based model for Multi-Objective (MO) power management for one MG to a multi-MG system. The basic idea here is to design an MG-wide distributed bargaining framework, using Nash Bargaining Solution (NBS) [10], to obtain a fair and Pareto-optimal solution to the power management problem. We have employed a distributed optimization approach (using the Distributed Sub-Gradient Algorithm (DSGA) [11] [12]) to implement a networked decision system. Hence, a multi-MG-system-wide MO optimization problem is solved through a distributed optimization model. The proposed model consists of three levels, as shown in Fig. 1. At the lowest level, the control agents of the micro-sources within each MG interact with each other to pursue the MG-wide objectives while satisfying the MG-wide constraints. At the upper level, the main control agents of the MGs at the Point of Common Coupling (PCC) interact with each other (and with the lower level control agents of the micro-sources of their own MG) to satisfy the multi-MG-level constraint of power balance. The upper level communication structure is sparser than the lower level interaction topology due to lower number of agents involved, as demonstrated in Fig. 1. This sparsity implies lower communication overhead which also permits data-privacy and data-ownership at individual MG level. While the lower level agents do not participate in the upper level bargaining process directly, the outcome of the lower level process is affected by the upper level negotiations. DSGA

K. Dehghanpour, and H. Nehrir are with the Department of Electrical and Computer Engineering, Montana State University, Bozeman, MT 59717 USA (e-mail: Kaveh.dehghanpour@msu.montana.edu; hnehrir@montana.edu).

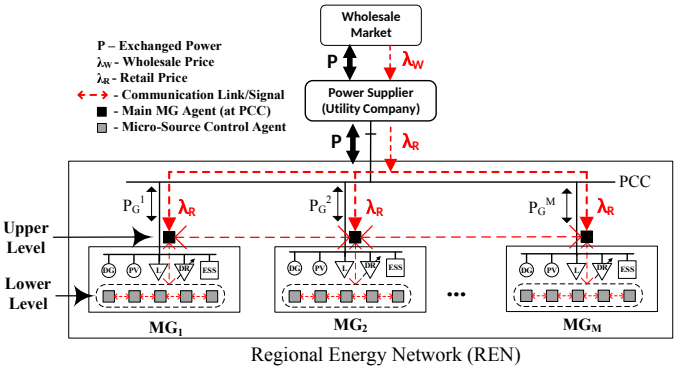

Fig. 1. Interaction structure of the proposed model.

is employed to implement these two levels of distributed bargaining. Given that the concept of NBS is adopted from the area of cooperative game theory [10], the cluster of MGs act as a cooperative community of players trying to reach a fair and optimal resource allocation. At the third and the highest level of the model, a power utility company acts as a retail market agent for the cluster of the MGs. The utility company facilitates power exchange between the distribution system and the wholesale market, by setting the retail energy price for the MGs. Hence, a dynamic pricing mechanism is adopted by the utility company to pursue its own objectives. Basically, the goal of the utility company is to indirectly control the outcome of the lower-level bargaining process to its own benefit.

The dynamic pricing procedure is based on our previous work in [13]. However, in [13] only a specific type of residential load was considered for the Day-Ahead (DA) retail market. In this paper, we expand the pricing model of [13] to include more active micro-sources at both the DA and Real-Time (RT) retail markets. At the DA stage the objective of the utility company is to maximize its profit based on the forecasted state of the system, subject to certain constraints, employing DA retail pricing. However, as we get closer to RT operation of the system, due to variations in system states (e.g., forecast errors, RT islanding scenarios, system failure) deviations from the DA schedule can occur. In this paper, we assume that at the RT stage the objective of the utility company is to minimize these deviations through RT retail pricing (i.e., any mismatch between the DA and RT power schedules are penalized in the regulation market.) Hence, the utility company's learned model is embedded within its DA and RT optimization problems to obtain the optimal retail price signals at those stages. Given the distributed, bi-directional and price-based nature of the decision model, we can argue that the overall methodology falls under the category of transactive control [14].

In summary, the main contributions of the paper are as follows:

- Employing the concept of NBS to address the cooperative and MO nature of the problem of resource allocation among multiple MGs. The NBS is cooperatively obtained by the MGs using a distributed optimization method (DSGA) without the need for a central controller. Hence, the MG agents are able to reach a consensus at any given retail price without the need for a central coordinator.
- The decision model at the MG level (excluding the utility company) is decomposed into two sub-layers to obtain a sparse communication network and reduce the communication overhead (the overall interaction architecture of the model is shown in Fig. 1)
- At the highest level (i.e., third level), a novel iterative retail pricing mechanism is introduced to be used by a utility company, based on a machine learning approach. Retail prices are obtained at different time stages (DA and RT) using a model learning procedure, through which the utility company estimates the price-responsivity of the MGs without having direct access to their decision model and private data.

The rest of the paper is constructed as follows: in Section II the overall structure of the MO distributed bargaining framework for the cluster of cooperative MGs is discussed. The decision problem of the utility company and its solution technique are presented in Section III. The results of the numerical experiments are shown and discussed in Section IV. The conclusions of the paper are presented in Section V.

II. Multi-MG Distributed Bargaining

In this section, the MO distributed bargaining mechanism (defining the first two levels of the decision model) is discussed. A rolling horizon optimization scheme, [15], is employed in RT to solve the distributed optimization problem. In this scheme, at each time instant (t) the power management problem is solved for a certain look-ahead time ($t+T$), based on the realized and forecasted values for renewable energy resources and the load, where T denotes the length of the decision horizon. The decision horizon is divided into H time steps (Δt). The forecast errors (for the renewable generation and non-controllable loads) are represented through Gaussian probability distribution functions selected according to [16] and [17]. Note that in this paper, we assume that the renewable energy sources of all the MGs are controlled through a maximum power point tracking mechanism, therefore, always generating maximum available power. This implies that the renewable power does not appear as a decision variable in the optimization problem.

A. Objective Functions and Constraints

Each MG is modeled as a community of cooperative micro-sources with different sets of objective functions and constraints, where each micro-source is controlled by its control agent. Each MG is assumed to be equipped with the following micro-sources (some of which are non-controllable): Photo-Voltaic (PV) power source, thermal Dispatchable Generation (DG) unit, Energy Storage System (ESS), fixed (non-controllable) load, and controllable Demand Response (DR) resources (i.e., curtailable loads). The following objective functions are considered for the dispatchable micro-sources of each MG. The objective functions are denoted as $U^m_{j,i}$,

indicating the j^{th} objective of the i^{th} micro-source of the m^{th} MG.

$$U^m_{1,1} = \sum_{t=1}^{H}\{-P^m_G(t)\lambda_R(t) - (a^m \cdot P^m_{DG}(t)^2 + b^m \cdot P^m_{DG}(t) + c^m)\} \quad (1)$$

$$U^m_{2,1} = \frac{1}{H} \cdot \sum_{t=1}^{H}\{\frac{k \cdot P^m_{DG}(t)}{a^m \cdot P^m_{DG}(t)^2 + b^m \cdot P^m_{DG}(t) + c^m}\} \quad (2)$$

$$U^m_{1,2} = \frac{1}{H} \cdot \sum_{t=1}^{H}\{\lambda_R(t) \cdot P^m_f(t) \cdot (1 - e^{-\omega^m (P^m_f(t) - P^m_C(t))})\} \quad (3)$$

$$U^m_{2,2} = \sum_{t=1}^{H}\{-P^m_C(t)\lambda_R(t)\} \quad (4)$$

$$U^m_{1,3} = \sum_{t=1}^{H}\{-(P^m_G(t))^2\} \quad (5)$$

where, $U^m_{1,1}$ and $U^m_{2,1}$ represent the two objectives of the DG agent of the m^{th} MG, denoting profitability of local power generation and average efficiency of operation, respectively. Here, $P^m_G(t)$ is the m^{th} MG's overall exchanged power with the distribution system (under the retail price $\lambda_R(t)$), with $P^m_G \leq 0$ representing power export to the grid and $P^m_G \geq 0$ implying power import from the grid. Also, Coefficients a^m, b^m, and c^m define the quadratic cost function of the DG [18], with $P^m_{DG}(t)$ denoting the output power of the DG unit. Two objective functions, $U^m_{1,2}$ and $U^m_{2,2}$ are also considered for the curtailable DR resources, representing a concave penalty function for load reduction, [19], and cost-savings function, respectively. Hence, deviations from the target (forecasted) fixed load value ($P^m_f(t)$) are penalized through $U^m_{1,2}$, based on the aggregate participation propensity of consumers, defined by ω^m for the m^{th} MG (with $P^m_C(t)$ denoting the aggregate operating power of the curtailed load). Finally, $U^m_{1,3}$ is the objective function considered for the main MG agent (of the m^{th} MG) to encourage self-sufficiency and avoid over-loading and congestion at the MG's PCC [20]. As shown in equations (1)-(5), the objective functions are defined as the summation/average over the whole decision window. However, in general only the optimal outcomes for the immediate time step within the decision window are used for power management and the rest are discarded or used for initialization in the future rounds of bargaining as the decision window rolls along time.

Apart from the introduced objective functions, the following constraints are considered for the control agents within each MG:

$$P^{min,m}_{DG} \leq P^m_{DG}(t) \leq P^{max,m}_{DG} \quad (6)$$

$$\frac{\mid P^m_{DG}(t) - P^m_{DG}(t-1) \mid}{\Delta t} \leq GRC^m \quad (7)$$

$$P^{min,m}_{ESS} \leq P^m_{ESS}(t) \leq P^{max,m}_{ESS} \quad (8)$$

$$SOC^m(t) = SOC^m(t-1) - \frac{\Delta t}{E_{max,m}} \cdot P^m_{ESS}(t) \quad (9)$$

$$SOC^{min,m} \leq SOC^m(t) \leq SOC^{max,m} \quad (10)$$

$$P^{min,m}_C \leq P^m_C(t) \leq P^{max,m}_C \quad (11)$$

$$P^{min,m}_G \leq P^m_G(t) \leq P^{max,m}_G \quad (12)$$

$$P^m_{DG}(t) + P^m_{PV}(t) + P^m_{ESS}(t) + P^m_G(t) + P^m_C(t) = P^m_f(t) \quad (13)$$

where, constraints (6) and (7) define the minimum/maximum generation limits ($P^{min,m}_{DG}$, $P^{max,m}_{DG}$) and the Generation Rate Constraint (GRC) of the DG control agent (for the m^{th} MG), which defines the ramping speed of the units. The ESS is also equipped with a control agent to enforce constraints (8), (9), and (10), which define the minimum/maximum power boundaries ($[P^{min,m}_{ESS}, P^{max,m}_{ESS}]$), and the State Of Charge (SOC) limits ($[SOC^{min,m}, SOC^{max,m}]$). $P^m_{ESS}(t)$ and $E_{max,m}$ denote the power output and the energy capacity of the ESS unit of the m^{th} MG. Constraint (11) maintains the curtailed load power between its minimum and maximum limits ($[P^{min,m}_C, P^{max,m}_C]$). Note that curtailable load resources are available only at specific time intervals, not always. The congestion constraint is shown in (12) to keep the exchanged power of each MG at the PCC within the permissible boundaries ($[P^{min,m}_G, P^{max,m}_G]$). Finally, the MG-wide power balance constraint is shown in (13) for the m^{th} MG. Note that in this equation, $P^m_{PV}(t)$ denotes the power output of the PV resource of the MG at time t (for the m^{th} MG).

While constraints (6)-(13) are maintained at the lowest level of the bargaining model by the control agents of the micro-sources of each MG, the multi-MG-system-wide power balance constraint, including all the MGs should also be considered in the bargaining process:

$$P^{max}_{Ex} \leq \sum_{m=1}^{M} P^m_G(t) \leq P^{max}_{Im} \quad (14)$$

where, M denotes the number of MGs. Hence, through (14) the total exchanged power of the MGs with the utility company is kept within the maximum export/import limit boundaries ($[P^{max}_{Ex}, P^{max}_{Im}]$). In general, the power flow constraints on the distribution network, connecting the MGs, can be introduced in the optimization problem using DC power flow approximation, as described in [21]:

$$\boldsymbol{P^{min}_l} \leq \{\boldsymbol{P_l} = \boldsymbol{H_N} \cdot \boldsymbol{P_G}\} \leq \boldsymbol{P^{max}_l} \quad (15)$$

where, $\boldsymbol{H_N}$ represents the matrix of shift factors for the distribution network [21], $\boldsymbol{P_l}$ denotes the power flow vector of the distribution network, and $\boldsymbol{P_G}$ is the vector of power export/import of the MGs (i.e., $\boldsymbol{P_G} = [P^1_G ... P^M_G]^T$). $\boldsymbol{P^{min}_l}$ and $\boldsymbol{P^{max}_l}$ define the minimum and maximum flow limit vectors on the lines of the network, respectively. Mathematically, the constraint (14) itself is a special case of the constraint (15).

Note that except for the control agents of MGs at the PCC (which are in charge of maintaining the constraints related to variables $P^m_G(t)$), the control agents of the micro-sources of MGs are "unaware" of the system-wide power balance and the network power flow constraints ((14) and (15)). However, these constraints affect the operating point of the micro-sources indirectly. In this way, the bargaining procedure is divided into two levels (which take place simultaneously): at the lower level, a distributed MO optimization problem is solved, through internal bargaining of all micro-source

control agents of each MG (with objective functions (1)-(5), subject to local MG-wide constraints (6)-(13)). Hence, this layer represents the most local portion of the decision model. At the upper level, the system-wide power balance constraints (14) (and (15)) are maintained through inter-MG negotiations. This functional separation within the multi-level bargaining structure leads to reduction in communication overheads and a sparse system-wide communication network, hence increasing the solution speed. Therefore, while at the lower level, the control agents of the micro-sources of each MG can enjoy full connectivity with each other, at the upper level, only the main control agents of the MGs at the PCC need to be connected to each other. Basically, the upper layer shields the lower layer agents from the inter-MG/global communication by eliminating unnecessary interaction links. As will become clear in the next subsection, from the perspective of the computational process (NBS and DSGA), there is no distinction between the lower and upper layers. Both of these layers are part of the same optimization problem (NBS), which is solved using DSGA, through a given communication network.

To summarize, the vectors of objective functions and constraint sets of the control agents within each MG are shown below (in this paper, vector and matrix quantities are shown in bold letters):

1) DG agent: $\boldsymbol{U_1^m} = [U_{1,1}^m \; U_{2,1}^m]^T$ and $X_1 = \{(6) \cap (7) \cap (13)\}$.
2) DR agent: $\boldsymbol{U_2^m} = [U_{1,2}^m \; U_{2,2}^m]^T$ and $X_2 = \{(11) \cap (13)\}$.
3) PCC agent: $\boldsymbol{U_3^m} = [U_{1,3}^m]^T$ and $X_3 = \{(12) \cap (13) \cap (14)\}$.
4) ESS agent: $\boldsymbol{U_4^m} = \emptyset$ and $X_4 = \{(8) \cap (9) \cap (10) \cap (13)\}$.

where, X_i denotes the feasible decision region of the i^{th} agent. Note that each agent has access to a private set of objective functions and a number of constraints, some of which are common among the agents (e.g., MG-wide power balance constraint). In the next subsection, the distributed optimization algorithm is described in details.

B. Distributed Optimization Algorithm

The concept of NBS [10] is employed to obtain a "fair", unique, and Pareto-optimal solution to the MO power management problem of the multi-MG system. Another advantage of NBS is that it can be obtained using a fully distributed computational process, within an agent-based framework. Hence, NBS provides a solution to the bargaining problem of a community of "cooperative" agents (i.e., cooperative MGs). A detailed description of NBS can be found in [10] [9].

The original MO power management problem of the multi-MG system is as follows:

$$\begin{aligned} &\max_{\boldsymbol{P}} \{U_{1,1}^1, U_{2,1}^1, U_{1,2}^1, U_{2,2}^1, U_{1,3}^1, ..., \\ &U_{1,1}^m, U_{2,1}^m, U_{1,2}^m, U_{2,2}^m, U_{1,3}^m\}, \\ &s.t. \; (6)-(15), \forall m \end{aligned} \tag{16}$$

where, $\boldsymbol{P}$ is the vector of decision variables, consisting of the power of controllable micro-sources of all the MGs (including the exchanged power values with the main grid) for the look-ahead time in which the power management problem is solved. The objective functions in (16) are concave and the feasibility region (constraints of (16)) is convex [22]. Thus, NBS is well-defined [10], and can be obtained as follows:

$$\begin{aligned} &\max_{\boldsymbol{P}} \{\sum_{m=1}^{M} \sum_{i=1}^{N_m} \log(\prod_{j=1}^{O_i^m} (U_{j,i}^m - d_{j,i}^m))\}, \\ &s.t. \; (6)-(14), \forall m \end{aligned} \tag{17}$$

where, N_m denotes the number of control agents within the m^{th} MG and O_i^m defines the number of objective functions of the i^{th} control agent in the m^{th} MG. Also, $d_{j,i}^m$'s represent the disagreement points of the bargaining process (i.e., worst case scenarios) [10]. Optimization problem (17) has a distributed sum structure, which can be written as:

$$\begin{aligned} &\min_{\boldsymbol{x_1}, ..., \boldsymbol{x_N}} \{\sum_{i=1}^{N} f_i(\boldsymbol{x_i})\}, \\ &s.t. \; \boldsymbol{x_i} \in X_i \end{aligned} \tag{18}$$

where, $\boldsymbol{x_i}$ denotes the decision vector of the i^{th} agent (with N being the number of agents). The cost function for each agent is represented by $f_i(\boldsymbol{x_i})$. For the NBS-based power management problem at hand, the decision vector of each agent is the power vector of the micro-sources in the system (i.e., $\boldsymbol{x_i} = \boldsymbol{P_i}$) and the cost function is as follows:

$$f_i(\boldsymbol{P_i}) = -\log(\prod_{j=1}^{O_i^m} (U_{j,i}^m - d_{j,i}^m)). \tag{19}$$

As shown in [11] and [12], problems of the form (18) can be solved using the distributed optimization technique, DSGA. Employing the DSGA and applying it to (17), the distributed cooperative bargaining framework for obtaining the NBS is obtained. At each iteration of the algorithm the following steps are performed by each control agent:

- **Step I:** at the k^{th} iteration of the algorithm, each agent receives the estimated solution vectors of its neighboring agents.
- **Step II:** the i^{th} agent performs a weighted averaging operation (with weights a_i^l) over the received signals from its neighboring agents (including its own estimated solution):

$$\boldsymbol{\omega_i(k)} = \sum_{l=1}^{Ne_i} a_i^l \boldsymbol{P_l(k)} \tag{20}$$

  where, Ne_i denotes the i^{th} agent's number of neighboring agents (including the i^{th} agent).
- **Step III:** at this step, each agent performs a gradient descent operation, as follows:

$$\boldsymbol{v_i(k)} = \boldsymbol{\omega_i(k)} - \alpha_k \cdot \nabla_{\boldsymbol{P_i}} f_i(\boldsymbol{P_i(k)}) \tag{21}$$

  where, α_k is a time-varying weight factor and is selected as $\alpha_k = \frac{\gamma}{k+1}$, with γ acting as a tunnable parameter of the model. The gradient of the cost function for the NBS formulation (17) is obtained as follows:

$$\nabla_{\boldsymbol{P}} f_i(\boldsymbol{P}) = -\begin{bmatrix} \frac{\partial U^m_{1,i}}{\partial P_1} & \cdots & \frac{\partial U^m_{O^m_i,i}}{\partial P_1} \\ \vdots & \ddots & \vdots \\ \frac{\partial U^m_{1,i}}{\partial P_L} & \cdots & \frac{\partial U^m_{O^m_i,i}}{\partial P_L} \end{bmatrix} \begin{bmatrix} \frac{1}{U^m_{1,i}-d^m_{1,i}} \\ \vdots \\ \frac{1}{U^m_{O^m_i,i}-d^m_{O^m_i,i}} \end{bmatrix} \tag{22}$$

- **Step IV:** each agent projects the outcome of Step II into its private feasible region (given in Section II) to update its estimated solution for the next iteration:

$$\boldsymbol{x_i(k+1)} = \Pi_{X_i}\{\boldsymbol{v_i(k)}\} \tag{23}$$

where, Π_{X_i} defines the projection operation into the set X_i. Note that the projection operation is a convex quadratic programming problem [22], which is formulated as follows:

$$\begin{aligned} \Pi_{X_i}\{\boldsymbol{v_i(k)}\} = \arg\min_{\boldsymbol{y}} \|\boldsymbol{y} - \boldsymbol{v_i(k)}\| \\ s.t.\ \boldsymbol{y} \in X_i \end{aligned} \tag{24}$$

where, $\|.\|$ is the Euclidean norm.

- **Step V:** The agents send their updated estimated solutions (i.e., $\boldsymbol{x_i(k+1)}$) to their neighbors.

III. Utility Company's Decision Model

At the highest level of the decision model, the utility company which acts as a mediator agent between the wholesale market and the cluster of cooperative MGs performs the two following steps:

- **Model Development:** The utility company develops a model to assess the aggregate price-sensitivity of the MGs (i.e., system identification). Note that the utility company does not have direct access to the decision problem of the MG agents. Price signals ($\boldsymbol{\lambda_R}$) are sent to the main MG agents and the estimated power export/import signals are received back from the MGs (as feedback signals). Based on these interactions a "learning" procedure is executed in which a price-sensitivity model (denoted as Γ) is fit to the response of the MGs (i.e., $\boldsymbol{P} = \Gamma(\boldsymbol{\lambda})$). In this paper, we have employed a multiple linear regression strategy for model development [13]:

$$\boldsymbol{P_a} = \boldsymbol{A}\boldsymbol{\lambda_R} + \boldsymbol{P_0} \tag{25}$$

where, $\boldsymbol{\lambda_R}$ is the retail price vector, matrix $\boldsymbol{A}$ and vector $\boldsymbol{P_0}$ are the time-varying parameters of the model that are learned through QR-decomposition [23]. $\boldsymbol{P_a}$ represents the aggregate sold/bought power from the cluster of MGs. Hence, at each iteration of the learning process the utility company "excites" the MGs with a price signal, which serves as an input data sample in the model. The aggregate feedback power signal (the aggregate of signals received from the main MG agents) acts as an output data sample in the learning process. After enough data samples are collected to ensure that the problem of model overfitting is avoided, the learned model is used by the utility company for future use. A detailed formulation of (25) is given below:

$$\begin{bmatrix} \sum_{m=1}^{M} P^m_G(1) \\ \vdots \\ \sum_{m=1}^{M} P^m_G(H) \end{bmatrix} = \begin{bmatrix} a_{11} & \cdots & a_{1H} \\ \vdots & \ddots & \vdots \\ a_{H1} & \cdots & a_{HH} \end{bmatrix} \begin{bmatrix} \lambda^1_R \\ \vdots \\ \lambda^H_R \end{bmatrix} + \begin{bmatrix} P^1_0 \\ \vdots \\ P^H_0 \end{bmatrix} \tag{26}$$

- **Retail Price Generation:** Based on the learned model, the utility company calculates the optimal retail price to achieve its own objectives. Two objective functions are considered in this paper, corresponding to the two stages of the market: at the DA stage the objective of the utility company is to maximize its profit through sale/purchase of power to/from the MGs, using the forecasted values for different variables in the system. Hence, a DA aggregate power profile is obtained from the MGs, based on the optimal DA retail prices, which is then submitted to the wholesale market. However, in RT due to the changes in the system variables and structure (e.g., prediction error, MG islanding, etc.) deviations from the DA schedule could occur. At the RT stage, the goal of the utility company is to fulfill the submitted DA power profile, using RT retail pricing (computed by the utility company) in order to minimize this deviation. Hence, we assume that the priority of the utility company is to compensate the deviations between the total DA and RT aggregate power of the MGs (any deviation is penalized in the RT wholesale regulation market.)

The Optimization problems corresponding to utility company's decision model at the DA and RT stages are as follows:

DA Retail Pricing: The objective function of the utility at this stage is to maximize the DA profit level from power exchange.

$$\begin{aligned} \min_{\boldsymbol{\lambda_{R,DA}}} \{ & -\boldsymbol{\lambda^T_{R,DA}} \cdot \boldsymbol{A} \cdot \boldsymbol{\lambda_{R,DA}} + (\boldsymbol{\lambda^T_{W,DA}} \cdot \boldsymbol{A} - \boldsymbol{P^T_0})\boldsymbol{\lambda_{R,DA}} \\ & + (\boldsymbol{\lambda^T_{W,DA}} \cdot \boldsymbol{P_0})\}, \\ s.t. & \begin{cases} \boldsymbol{\lambda^{min}_{R,DA}} \preceq \boldsymbol{\lambda_{R,DA}} \preceq \boldsymbol{\lambda^{max}_{R,DA}} \\ (\boldsymbol{\lambda_{R,DA}} - \boldsymbol{\lambda_{W,DA}})^T \cdot \Gamma(\boldsymbol{\lambda_{R,DA}}) \leq \pi^{max}, \end{cases} \end{aligned} \tag{27}$$

where, $\boldsymbol{\lambda_{R,DA}}$ and $\boldsymbol{\lambda_{W,DA}}$ denote the DA retail and wholesale price vectors, respectively. Also, "$\preceq$" denotes the vector form of operator "$\leq$". The constraints of the optimization problem define the minimum/maximum boundaries on the price vector ($[\boldsymbol{\lambda^{min}_{R,DA}}, \boldsymbol{\lambda^{max}_{R,DA}}]$), and a maximum DA profit level for the retailer (i.e., π^{max}). Optimization problem (27) is a case of Quadratically Constrained Quadratic Programming (QCQP) [22].

RT Retail Pricing: At this stage, the objective function of the utility is to minimize the deviation between the aggregate RT power profile of the MGs and the scheduled DA plan ($\boldsymbol{P_{DA}}$, obtained from the DA stage) by obtaining optimal retail prices:

$$\begin{aligned} \min_{\boldsymbol{\lambda_{R,RT}}} \{\boldsymbol{\lambda_{W,RT}} \cdot \|\Gamma(\boldsymbol{\lambda_{R,RT}}) - \boldsymbol{P_{DA}}\|\}, \\ s.t.\ \boldsymbol{\lambda^{min}_{R,RT}} \preceq \boldsymbol{\lambda}_{R,RT} \preceq \boldsymbol{\lambda^{max}_{R,RT}} \end{aligned} \tag{28}$$

where, $\boldsymbol{\lambda_{R,RT}}$ and $\boldsymbol{\lambda_{W,RT}}$ are the RT retail and wholesale price vectors, respectively. The only constraint considered at

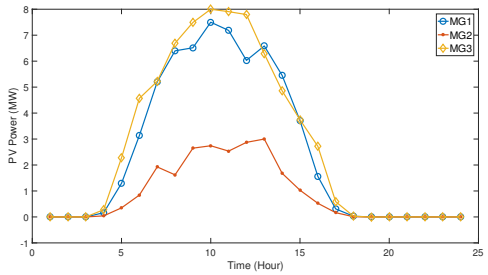

Fig. 2. PV power data for the different MGs.

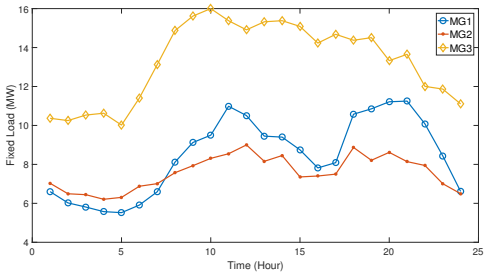

Fig. 3. Fixed load profiles of the different MGs.

this stage is to keep the price within its minimum/maximum boundaries ($[\boldsymbol{\lambda^{min}_{R,RT}}, \boldsymbol{\lambda^{max}_{R,RT}}]$). Fig. 1 shows the interaction structure of the retail market agent (utility company) with the wholesale market and the MG-based energy network.

IV. Simulation Results and Discussion

The proposed decision framework is tested in a power system with three MGs. Each MG is based on modified versions and variations of the IEEE 13-bus standard distribution network used in our earlier work [9]. The PV power profiles of different MGs are adopted from [24] and shown in Fig. 2. The fixed load data for the three MGs, shown in Fig. 3, are obtained from [25] and [26], and the wholesale DA and RT market prices are adopted from [27].

In the simulation experiment scenario we assume that all the three MGs participate in the DA retail market. However, in the RT stage, we assume a disturbance (one of the MGs is islanded from the distribution system for the whole day, performing internal single-MG bargaining as described in [9].) Based on this scenario, the numerical results are discussed in the rest of this section.

A. DA Stage: On the utility company's side, the learning process performed by the utility leads to low prediction errors, as can be seen in Fig. 4 (i.e., after a transient stage the utility company is able to predict the aggregate response of the MGs to the price signal with high accuracy using the developed model). The Mean Absolute Error (MAE) of power prediction reaches a value of 2% through the iterations. As the model development step is completed, the result of optimal pricing for the DA retail market is shown in Fig. 5. Also, the individual and aggregate exported power of the three MGs under the optimal DA retail prices are shown in Fig. 6. As is observed in these figures, the utility company "buys" power

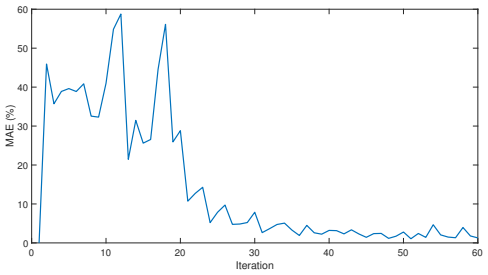

Fig. 4. Utility company's power prediction error.

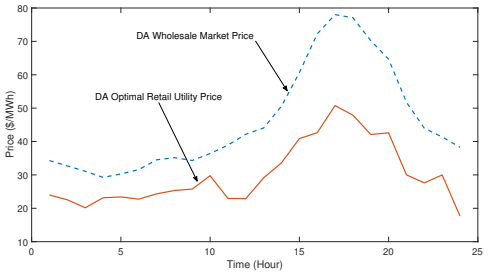

Fig. 5. DA wholesale/retail prices.

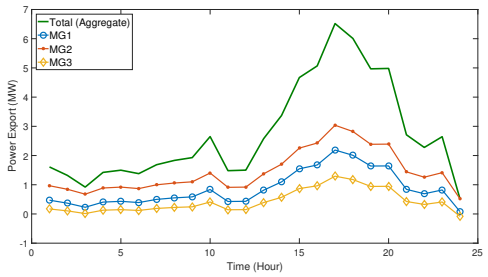

Fig. 6. MGs' power exchange with the utility company.

from the MGs at the optimal retail price and sells it on the DA wholesale market at a higher wholesale price (Fig. 5). Hence, the price-sensitivity of the distribution system leads to lower energy prices at the retail level compared to the wholesale level. Also, it can be seen that as the value of the retail price signal increases, the power export levels of the MGs increase as well (i.e., MGs "sell" more power to the utility company at higher retail prices).

The DA profit profile of the utility company is shown in Fig. 7. As can be seen in this figure, higher power exports to the wholesale market results in intervals of higher profit for the utility company. Also, the total profit level of the utility company for the whole day throughout the learning process (i.e., model development iterations) is demonstrated in Fig. 8. As is shown in this figure, the profit level of the utility company improves and reaches its maximum level, as the learning process produces a reliable model of the price-sensitivity of the MGs for the utility company.

The DA power profiles of the DG units of the MGs is shown in Fig. 9. As can be seen in this figure, the three DG units of the MGs provide a base load at the earlier hours of the day. But, at later hours, the DG units increase their power output due to higher retail price levels, which makes

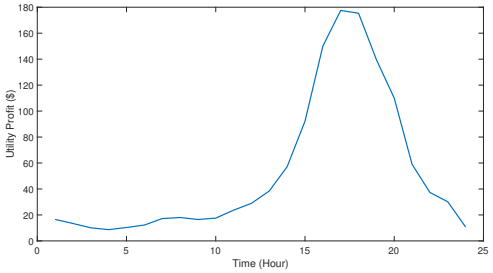

Fig. 7. Utility company's hourly profit profile.

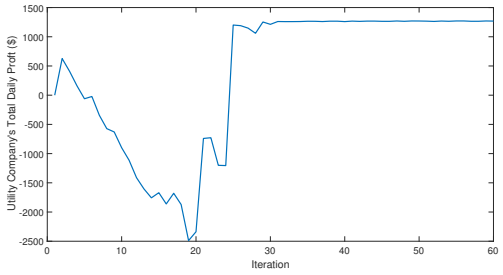

Fig. 8. Utility company's daily total profit profile throughout the learning process.

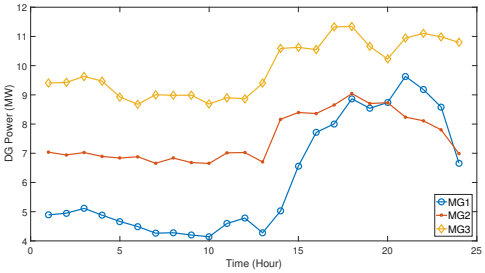

Fig. 9. DA DG power profile of the MGs.

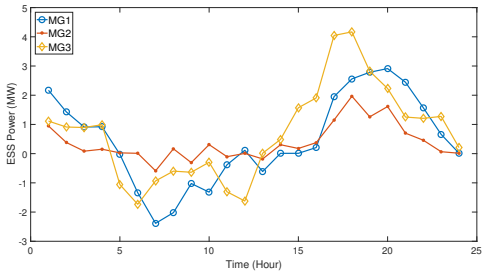

Fig. 10. DA ESS power profile of the MGs.

power generation more profitable. The same principle applies to the ESS units. As shown in Fig. 10, the ESS units are in charging state at earlier hours of the day with lower retail prices (negative power implies charging), and discharging state at the later hours during the high price interval. The stored energy profile (DA SOC) of the ESS units are shown in Fig. 11, along with the minimum/maximum allowable energy (SOC) limits ($[E^{min,m}, E^{max,m}]$). It can be observed that the bargaining process has maintained the stored energy levels of the ESS units within the acceptable ranges at all times. The total maximum available and the realized curtailable demand resources (for all MGs) are depicted in Fig. 12. While up to a maximum of 20% of the total fixed load is available for curtailment (at hours 19:00 and 20:00), the realized curtailment demand value reaches 11% of the total fixed load (at hours 19:00 and 20:00). This is well below the maximum available level (i.e., only about half of the available DR resources are employed at the peak demand hours.) All the MGs respond to the increase in the price signal, as shown in Fig. 6. However, since the MGs are not identical, the increase in the export levels are not equal, and depend on many factors, such as the local demand level of each MG (Fig. 3), generator ramping constraints, available PV power (Fig. 2), ESS capacity and storage level, etc. For instance, the DG unit of MG1 shows a considerable power output increase in the time span 15:00 20:00. While this increase is partly due to higher retail price (which makes local generation more profitable), it is also caused by higher load levels in MG1 during this time. On the other hand, the discharge rate of the ESS units in all the MGs increase considerably during the peak price time interval (Fig. 10), with MG3 showing the maximum increase in discharge power. In addition, the rate and duration of discharge partly depends on the available stored energy level and SOC constraints in the decision model (shown in Fig. 11).

B. RT Stage: As discussed previously, we assume that in RT, one of the MGs is islanded during the whole day. This scenario demonstrates the effectiveness of the proposed decision scheme in RT, under significant structural changes in the system. The aggregate power export level of the MGs to the wholesale market is shown in Fig. 13. As can be seen in this figure, if no corrective action is undertaken by the utility company a large power deficit will occur in RT, due to the islanding of an MG, which results in power generation deficit. However, by solving (28) and modifying (increasing) the RT retail prices, the utility company undertakes corrective action to minimize the power deficit by using other available resources in the grid-connected MGs. As is observed in Fig. 13, the corrected aggregate power profile of the remaining two MGs under the new RT price is nearly identical to the scheduled DA power profile, even though one of the MGs was islanded. Hence, using corrective action the power mismatch level drops from an overall value of 52.7% to 6% (Fig. 13). The optimal RT retail price that achieves this low level of

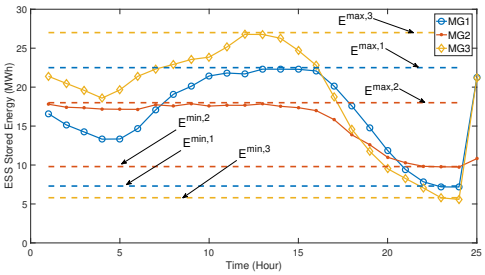

Fig. 11. DA ESS SOC profile of the MGs.

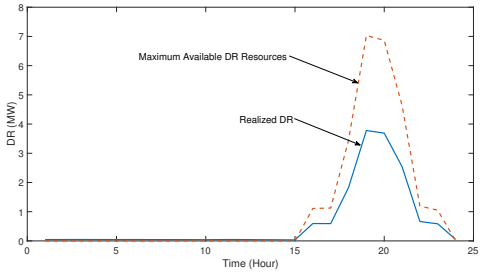

Fig. 12. DA curtailed aggregate load of the MGs.

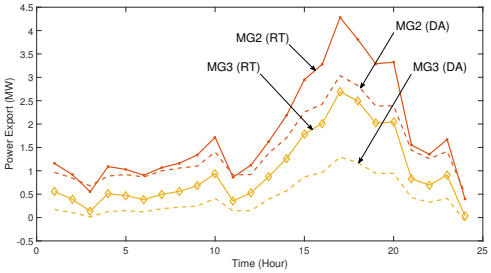

Fig. 15. Grid-connected MGs' DA and RT power export profiles.

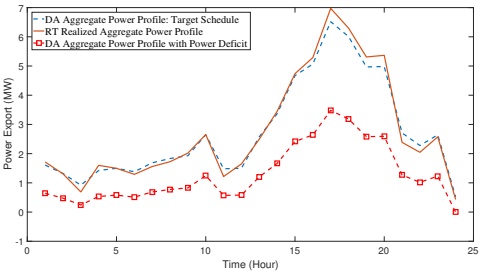

Fig. 13. Aggregate power profile of the system in RT.

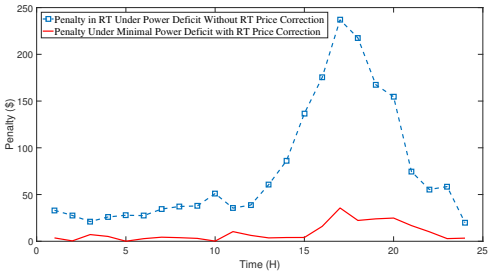

Fig. 16. Utility company's penalty level in the wholesale market.

power mismatch is shown in Fig. 14. As demonstrated in this figure, a considerable increase in the utility retail price is observed. In other words, the utility company increases the RT retail prices in order to incentivize the non-islanded MGs to produce more power to compensate for the power deficit caused by the islanded MG, and minimize the power mismatch between the RT aggregate profile and the DA power schedule. Hence, the utility is able to find the "correct" RT retail price signal to achieve its objective by indirectly controlling the behavior of the MGs. The changes in power exports of MG2 and MG3 (that are grid-connected) to the utility compared with their DA schedule are shown in Fig. 15. As can be seen here, both MGs increase their net output power in response to the new price signal to compensate for the lost power export of the islanded MG, which implies a more flexible and active distribution system with higher levels of controllability.

The penalty levels for the power mismatch values in the RT wholesale market, are shown in Fig. 16 for two cases: 1) no corrective action is undertaken in RT by the utility company (i.e., maximum penalty), and 2) corrective RT retail pricing is performed to minimize the power mismatch. Note that the penalty levels define the monetary values paid by the utility company to the wholesale regulation market to compensate for the deviations from the DA power schedule. Here, a drop in the penalty level is also observed through optimal RT pricing. The penalty level drops from a total value of $1841.6 for the day under case 1 (which is above the utility company's total DA profit of $1307.2) to $214.8 for case 2, which implies an 88% improvement. Hence, the RT retail pricing scenario demonstrates the effectiveness of the proposed decision model in providing a safe and economically viable operation margin for different parties in the multi-MG system (including the utility company).

C. Discussion: In order to investigate the suitability of our proposed distributed optimization methodology for RT power management applications, we compared it with a conventional central optimization method available in MATLAB's optimization toolbox. Due to the convexity of the decision model, both the central and the proposed distributed optimization methods yield the exact same results. Fig. 17 shows the convergence of the two optimization methods for one round of bargaining, where, the global objective function of the

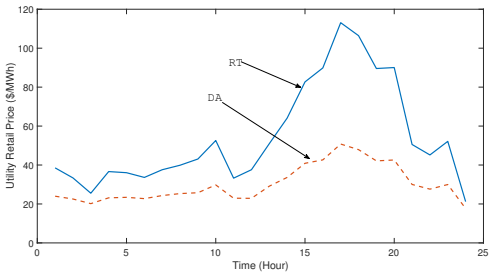

Fig. 14. Optimal RT retail prices.

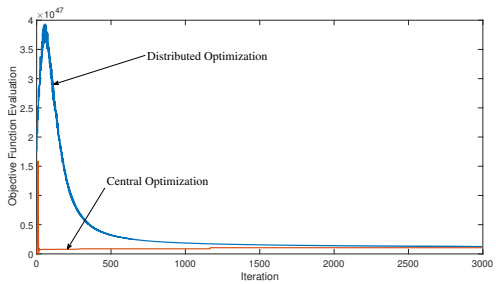

Fig. 17. Optimization convergence demonstration.

optimization problem (17) is evaluated at different iterations of the optimization solvers. As shown in the figure, the two methods converge to the same value in each round of bargaining. Although, the distributed optimization method has a longer transient period, its convergence time is much shorter. While our proposed distributed bargaining technique converged in around 15 minutes per round, the convergence of the central optimization took about one hour. This indicates that the conventional central optimization method has a much higher computational load per iteration, compared to our proposed distributed optimization technique.

We used one computer to perform the agent-based distributed MO optimization, whereas in practice different computers and computational resources are used for each agent to perform their tasks. This leads to even less computational delays compared to the case where all agents are implemented on the same machine. Also, note that by reducing the look-ahead time horizon of the algorithm (i.e., T) this computational time can be further improved. Hence, we believe that the proposed distributed bargaining technique is suitable for real-time applications in power systems.

V. Conclusion

In this paper, an agent-based hierarchical MO decision model is proposed to handle the power management problem of an energy network with multiple MGs. At the lower and upper levels of the model the cooperative cluster of MGs bargain with each other to reach a fair and Pareto-optimal solution, employing the concept of NBS within a distributed optimization framework. At the highest level, a utility company sets the retail prices for the MGs to achieve its own objective through power exchange with the MGs at the DA and RT market stages. The utility company is able to pursue its goals solely based on optimal energy pricing (through a machine learning technique) and without direct access to the internal control process of the MGs. The distributed and agent-based nature of the model eliminates the need for a central control, which leads to an automation system without a single point of failure. This also reduces the computational load of each control agent in the system, which makes the proposed decision model a suitable choice for wide-scale implementation in real-time.

References

[1] C. Yuen, A. Oudalov, and A. Timbus, "The provision of frequency control reserves from multiple microgrids," *IEEE Trans. Ind. Electron.*, vol. 58, no. 1, pp. 173–183, Jan. 2011.

[2] H. S. V. S. K. Nunna and S. Doolla, "Demand response in smart distribution system with multiple microgrids," *IEEE Trans. Smart Grid*, vol. 3, no. 4, pp. 1641–1649, Dec. 2012.

[3] ——, "Multiagent-based distributed-energy-resource management of intelligent microgrids," *IEEE Trans. Ind. Electron.*, vol. 60, no. 4, pp. 1678–1687, Apr. 2013.

[4] M. Marzband, N. Parhizi, M. Savaghebi, and J. M. Guerrero, "Distributed smart decision-making for a multimicrogrid system based on a hierarchical interactive architecture," *IEEE Trans. Energy Convers.*, vol. 31, no. 2, pp. 637–648, Jun. 2016.

[5] D. Wang, X. Guan, J. Wu, P. Li, P. Zan, and H. Xu, "Integrated energy exchange scheduling for multimicrogrid system with electric vehicles," *IEEE Trans. Smart Grid*, vol. 7, no. 4, pp. 1762–1774, Jul. 2016.

[6] Y. Wang, S. Mao, and R. M. Nelms, "On hierarchical power scheduling for macrogrid and cooperative microgrids," *IEEE Trans. Ind. Informat.*, vol. 11, no. 6, pp. 1574–1584, Dec. 2015.

[7] J. Lee, J. Guo, J. K. Choi, and M. Zukerman, "Distributed energy trading in microgrids: a game-theoretic model and its equilibrium analysis," *IEEE Trans. Ind. Electron.*, vol. 62, no. 6, pp. 3524–3533, Jun. 2015.

[8] D. Gregoratti and J. Matamoros, "Distributed energy trading: the multiple-microgrid case," *IEEE Trans. Ind. Electron.*, vol. 62, no. 4, pp. 2551–2559, Apr. 2015.

[9] K. Dehghanpour and H. Nehrir, "Real-time multiobjective microgrid power management using distributed optimization in an agent-based bargaining framework," *To Appear in IEEE Trans. Smart Grid*, 2016.

[10] M. Maschler, E. Solan, and S. Zamir, *Game theory*. New York: Cambridge University Press, 2013.

[11] A. Nedic and A. Ozdaglar, "Distributed subgradient methods for multi-agent optimization," *IEEE Trans. Automat. Control*, vol. 54, no. 1, pp. 48–61, Jan. 2009.

[12] A. Nedic, A. Ozdaglar, and P. A. Parrilo, "Constrained consensus and optimization in multi-agent networks," *IEEE Trans. Automat. Control*, vol. 55, no. 4, pp. 922–938, Apr. 2010.

[13] K. Dehghanpour, H. Nehrir, J. W. Sheppard, and N. C. Kelly, "Agent-based modeling of retail electrical energy markets with demand response," *To Appear in IEEE Trans. Smart Grid*.

[14] K. Kok and S. Widergren, "A society of devices: Integrating intelligent distributed resources with transactive energy," *IEEE Power and Energy Magazine*, vol. 14, no. 3, pp. 34–45, 2016.

[15] R. P. Behnke, C. Benavides, F. Lanas, B. Severino, L. Reyes, J. Llanos, and D. Saez, "A microgrid energy management system based on the rolling horizon strategy," *IEEE Trans. Smart Grid*, vol. 4, no. 2, pp. 996–1006, Jun. 2013.

[16] C. Yang, A. A. Thatte, and L. Xie, "Multitime-scale data-driven spatio-temporal forecast of photovoltaic generation," *IEEE Trans. Sustain. Energy*, vol. 6, no. 1, pp. 104–112, Jan. 2015.

[17] C. Guan, P. B. Luh, L. D. Michel, Y. Wang, and P. B. Friedland, "Very short-term load forecasting: wavelet neural networks with data pre-filtering," *IEEE Trans. Power Syst.*, vol. 28, no. 1, pp. 30–41, Feb. 2013.

[18] A. Pourmousavi, M. H. Nehrir, and R. K. Sharma, "Multi-timescale power management for islanded microgrids including storage and demand response," *IEEE Trans. Smart Grid*, vol. 6, no. 3, pp. 1185–1195, May 2015.

[19] Z. M. Fadlullah, D. M. Quan, N. Kato, and I. Stojmenovic, "GTES: an optimized game-theoretic demand-side management scheme for smart grid," *IEEE Syst. J.*, vol. 8, no. 2, pp. 588–597, Jun. 2014.

[20] M. Ross, C. Abbey, F. Bouffard, and G. Joos, "Multiobjective optimization dispatch for microgrids with a high penetration of renewable generation," *IEEE Trans. Sustain. Energy*, vol. 6, no. 4, pp. 1306–1314, Oct. 2015.

[21] D. R. Biggar and M. R. Hesamzadeh, *The Economics of Electricity Markets*. John Wiley & Sons, 2014.

[22] S. Boyd and N. Vandenberghe, *Convex optimization*. New York: Cambridge University Press, 2009.

[23] C. L. Lawson and R. J. Hanson, *Solving least squares problems*. New Jersey: Prentice-hall, 1974.

[24] "Electric Power Research Institute (EPRI): Distributed PV monitoring and feeder analysis - Jun. 2012," http://dpv.epri.com/measurement_data.html.

[25] NREL, "Randomized hourly load data for use with taxonomy distribution feeders," https://catalog.data.gov/harvest/object/, Nov. 2015.

[26] A. Hoke, R. Butler, J. Hambrick, , and B. Kroposki, "Steady-state analysis of maximum photovoltaic penetration levels on typical distribution feeders," *IEEE Trans. Sustain. Energy*, vol. 4, no. 2, pp. 350–357, Apr. 2013.

[27] "California independent system operator data," http://www.caiso.com/Pages/default.aspx.